RESEARCH PAPER

Small GTPases 2:3, 131-142; May/June 2011; © 2011 Landes Bioscience

# Impaired prenylation of Rab GTPases in the *gunmetal* mouse causes defects in bone cell function

Adam Taylor,[1] Emilie H. Mules,[2] Miguel C. Seabra,[2-4] Miep H. Helfrich,[1] Michael J. Rogers[1] and Fraser P. Coxon[1,*]

[1]Musculoskeletal Programme; Division of Applied Medicine; Institute of Medical Sciences; University of Aberdeen; Foresterhill, Aberdeen UK; [2]Department of Molecular Medicine; National Heart and Lung Institute; Imperial College; London, UK; [3]CEDOC da Faculdade de Ciência Médicas; Universidade Nova de Lisboa; Lisboa, Portugal; [4]Instituto Gulbenkian de Ciência; Oeiras, Portugal

**Key words:** osteoclast, bone resorption, bone, Rab, small GTPase, prenylation, gunmetal

**Abbreviations:** GGPP, geranylgeranyl diphosphate; GGTase, geranylgeranyl transferase; *gm/gm*, gunmetal; GTP, guanosine triphosphate; MCSF, macrophage-colony stimulating factor; μCT, micro computed tomography; N-BP, nitrogen-containing bisphosphonate; OPG, osteoprotegerin; OVX, ovariectomy; PBMC, peripheral blood mononuclear cell; PC, phosphonocarboxylate; PTH, parathyroid hormone; RANKL, receptor activator of NFκB ligand; RGGT, rab geranylgeranyl transferase; TEM, transmission electron microscopy; TRAP, tartrate-resistant acid phosphatase

Vesicular trafficking is crucial for bone resorption by osteoclasts, in particular for formation of the ruffled border membrane and for removal of the resultant bone degradation products by transcytosis. These processes are regulated by Rab family GTPases, whose activity is dependent on post-translational prenylation by Rab geranylgeranyl transferase (RGGT). Specific pharmacological inhibition of RGGT inhibits bone resorption in vitro and in vivo, illustrating the importance of Rab prenylation for osteoclast function. The *gunmetal* (*gm/gm*) mouse bears a mutation in the catalytic subunit of RGGT, causing a loss of 75% of the activity of this enzyme and hence hypoprenylation of several Rabs in melanocytes, platelets and cytotoxic T cells. We have now found that prenylation of several Rab proteins is also defective in *gm/gm* osteoclasts. Moreover, while osteoclast formation and cytoskeletal polarization occurs normally, *gm/gm* osteoclasts exhibit a substantial reduction in resorptive activity in vitro compared with osteoclasts from *+/gm* mice, which do not have a prenylation defect. Surprisingly, rather than the osteosclerosis that would be expected to result from defective osteoclast function in vivo, *gm/gm* mice exhibited a slightly lower bone mass than *+/gm* mice, indicating that defects in other cell types, such as osteoblasts, in which hypoprenylation of Rabs was also detected, may contribute to the phenotype. However, *gm/gm* mice were partially protected from ovariectomy-induced bone loss, suggesting that levels of Rab prenylation in *gm/gm* osteoclasts may be sufficient to maintain normal physiological levels of activity, but not pathological levels of bone resorption in vivo.

## Introduction

A healthy skeleton is maintained through bone remodelling, which involves the tightly regulated, opposing actions of bone-resorbing osteoclasts and bone-forming osteoblasts. Osteoclasts are multinucleated cells formed as a result of the fusion of monocyte/macrophage precursors[1] in response to the cytokines macrophage-colony stimulating factor (MCSF)[2] and receptor activator of NFκB ligand (RANKL), both of which are produced by osteoblasts.[3] During their activation, osteoclasts polarize their membrane into four distinct domains; bone resorption takes place at one of these domains, known as the ruffled border, as a result of the selective delivery of lysosomes to this membrane.[4] In later life, the delicate balance between osteoclast and osteoblast activity may be tipped in favor of excessive bone resorption by osteoclasts, leading to osteoporosis, a disease characterized by reduced bone mineral density and susceptibility to fracture. Accordingly, inhibiting osteoclast survival or function has become the major therapeutic strategy for maintaining bone mass in this disease.

Currently, the most widely-used anti-resorptive drugs are the nitrogen-containing bisphosphonates (N-BPs), which work by inhibiting the mevalonate pathway enzyme farnesyl diphosphate synthase.[5,6] This prevents the synthesis of the isoprenoids FPP and GGPP, thus preventing the post-translational prenylation of Ras, Rho and Rab GTPases that are essential for osteoclast function.[7,8] Interestingly, phosphonocarboxylate (PC) analogs of N-BPs, in which one of the phosphonate groups is replaced by a carboxylate group, do not inhibit farnesyl FPP synthase, but are specific inhibitors of Rab geranylgeranyltransferase (RGGT),

*Correspondence to: Fraser P. Coxon; Email: f.p.coxon@abdn.ac.uk
Submitted: 03/08/11; Accepted: 05/13/11
DOI: 10.4161/sgtp.2.3.16488

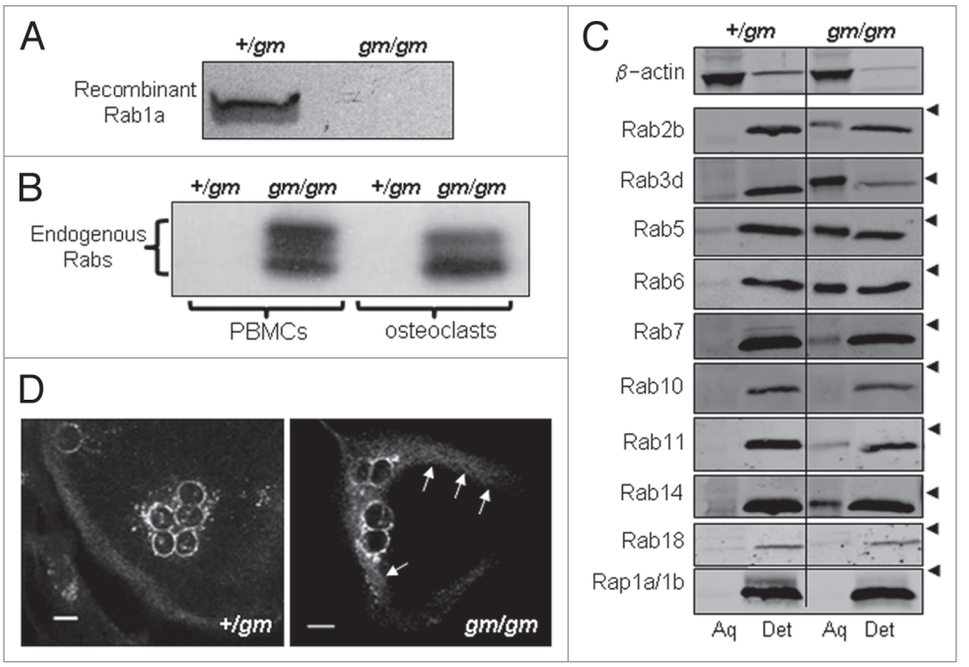


**Figure 1.** *gm/gm* osteoclasts have reduced RGGT activity and underprenylated Rabs. Endogenous RGGT activity in lysates of osteoclasts from *gm/gm* and *+/gm* mice was assessed by detecting the incorporation of [$^3$H]geranylgeranyl-disphosphate into recombinant Rab1 (A). Unprenylated Rabs in *gm/gm* and *+/gm* lysates were detected by assessing the incorporation of [$^3$H]geranylgeranyl-disphosphate on to Rab GTPases in the presence of recombinant RGGT (B). Osteoclasts were lysed in triton X-114 buffer and fractionated into aqueous and detergent phases, enabling the separation of unprenylated and prenylated Rabs, respectively, which were detected by protein gel blotting; arrowheads indicate the position of the 28 kDa marker (C). The cellular localization of endogenous Rab6 was visualized in osteoclasts from *gm/gm* and *+/gm* mice by immunostaining (D).

another enzyme of the mevalonate pathway that is specifically responsible for the prenylation of cysteine residues in characteristic motifs in the C-terminus of Rabs.[9] Since phosphonocarboxylates also inhibit bone resorption,[9-12] prenylation of Rabs is likely to be essential for the resorptive process, although the possibility that the phosphonocarboxylates inhibit bone resorption through mechanisms other than inhibition of RGGT cannot be excluded. However, it is clear that certain Rabs, including Rab7 [13] and Rab3d[14] are essential for vesicular trafficking to the ruffled border, the resorptive organelle of the osteoclast.

Convincing evidence for the dependence of certain cell types on prenylation of Rabs has come from studies of the naturally occurring *gunmetal* (*gm/gm*) mouse, which bears an autosomal recessive mutation in the catalytic α subunit of RGGT, resulting in an 75% reduction in RGGT activity.[15] Consequently, the geranylgeranylation of a subset of Rab proteins, in particular Rab27a, is reduced in melanocytes, megakaryocytes and platelets in these mice,[16,17] resulting in the characteristic greyish-black coat (hence the name *gunmetal*), extended bleeding time, thrombocytopenia and reduced platelet granule contents.[18,19] Despite the decreased RGGT activity, defective prenylation of Rab proteins is not seen in most other tissues, therefore helping to explain the restricted phenotype of these mice.[16] Moreover, in those tissues that are affected, the effects seem to be mainly the result of defective prenylation of Rab27a, which is expressed at extremely high levels in the affected tissues. Therefore one hypothesis for the limited phenotype is that the impaired RGGT activity cannot keep pace with the high prenylation demand for this Rab.[16] This explanation alone is insufficient though, as it has become clear that Rabs expressed at similar levels can be found differentially underprenylated, indicating that other factors, such as intrinsic GTP hydrolysis rate, may also play a role in making Rab27 particularly susceptible to underprenylation.[20] However, unlike the cell types known to be compromised in the *gm/gm* mouse, osteoclasts do not express high levels of Rab27a or Rab27b, despite the former being present in precursor cells (Coxon FP and Seabra MC, unpublished data). Despite this, parallels can be drawn between osteoclasts and the affected melanocytes and platelets, since they are all dependent on the ability to coordinate biogenesis, transportation and fusion of lysosome related organelles (LROs) with the plasma membrane in order to evacuate their contents,[4,21] which in the case of osteoclasts is the acid and proteases that mediate dissolution of bone mineral and digestion of type I collagen, respectively.

In this study, therefore, we have utilized the *gm/gm* mouse to clarify the importance of Rab prenylation levels for osteoclast function. The prenylation of a number of Rab proteins was found to be defective in osteoclasts derived from the *gm/gm* mice, and these cells also exhibited a substantial reduction in resorptive activity in vitro compared with heterozygote controls, despite normal osteoclast formation and cytoskeletal polarization. Surprisingly, rather than the osteosclerosis that would be expected to result from defective osteoclast function in vivo, the mice exhibited a slightly lower bone mass than heterozygote controls, indicating that other compensatory factors or defects in other cell types, such as osteoblasts, may affect the skeletal phenotype of these mice.

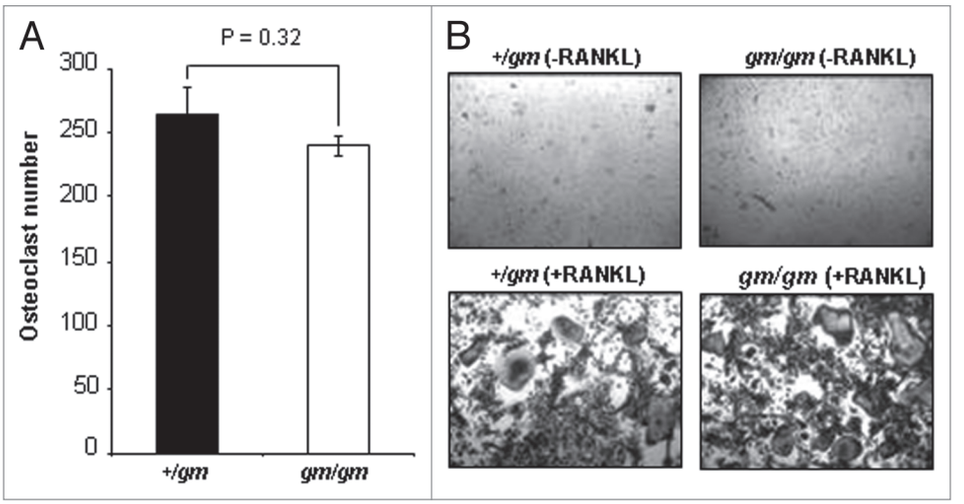


**Figure 2.** Osteoclastogenesis from *gm/gm* bone marrow in vitro is normal. Marrow from *+/gm* and *gm/gm* mice was seeded into flasks and incubating with MCSF for 24 h prior to transfer into 96-well plates for further culture in the presence of RANKL for 4 d. Osteoclast were identified as having three or more nuclei and being positive for TRAP staining (B) and quantified at the end of the culture period (A).

## Results

**Osteoclasts from *gm/gm* mice contain a pool of unprenylated proteins.** Dysfunctional prenylation of Rabs has been reported in a number of *gm/gm* tissues, including platelets and melanocytes, as a result of the reduced RGGT activity.[15,16] As expected, endogenous RGGT activity in lysates of osteoclasts generated from *gm/gm* mouse marrow, assessed by analyzing prenylation of recombinant Rab1 with [$^3$H]GGPP, was dramatically reduced compared with lysates from *+/gm* osteoclasts (**Fig. 1A**). Under physiological conditions, where RGGT function is normal, Rabs exist predominantly in the prenylated form. Indeed, we found no incorporation of [$^3$H]GGPP into Rabs in lysates of osteoclasts or PBMCs from *+/gm* mice, indicating a lack of endogenous substrates for prenylation i.e., the intracellular pool of Rabs were fully prenylated, at least within the limitations of sensitivity of this assay. By contrast, we found extensive incorporation of [$^3$H]GGPP into Rab proteins of several different molecular weights in both osteoclast and PBMC lysates from the *gm/gm* mice, clearly indicating the presence of unprenylated pools of numerous Rabs that were substrates for the in vitro prenylation (**Fig. 1B**).

The process of prenylation makes Rabs more lipophilic, enabling the use of triton X-114 fractionation to separate the prenylated forms (detergent-rich phase) from the unprenylated forms (aqueous phase).[10] Protein gel blot analysis using antibodies to specific Rabs indicated that all the Rabs analyzed existed almost entirely in the prenylated form in *+/gm* osteoclasts. However, a substantial proportion of several of these Rabs existed in the unprenylated form in *gm/gm* osteoclasts (percentage unprenylated indicated in parentheses): Rab2B (35%), Rab3d (73%) Rab5 (42%), Rab6 (40%), Rab7 (14%) and Rab14 (27%) (**Fig. 1C**). By contrast, the proportion of unprenylated Rab10 or Rab18 detected in *gm/gm* osteoclasts was no different from the *+/gm* osteoclasts. As a control, we used Rap1a, which is prenylated by GGTase I rather than RGGT, and was detected entirely in the prenylated form in both *gm/gm* and *+/gm* osteoclasts (**Fig. 1C**). Using immunostaining we found that Rab6 exhibited reduced localization to the Golgi and slightly increased cytoplasmic localization in *gm/gm* osteoclasts compared with *+/gm* osteoclasts (**Fig. 1D**), consistent with an accumulation of the unprenylated form of this Rab.

**Osteoclast resorptive activity, but not osteoclastogenesis, is compromised in *gm/gm* osteoclasts.** There were no differences in the ability of TRAP positive, multinucleated osteoclasts to form from the bone marrow macrophages of g*m/gm* and *+/gm* mice when treated with RANKL and MCSF (**Fig. 2**); a similar result was obtained when the osteoclasts were formed using dentine as the substrate (**Fig. 3C**). In addition, in the cultures on dentine, similar numbers of osteoclasts were able to polarize their cytoskeleton into a characteristic "actin ring," which creates the sealing zone within which bone resorption takes place (**Fig. 3A and B**). However, the *gm/gm* osteoclasts were defective in their resorptive activity, exhibiting a significant 50% reduction in resorption pit area on dentine, as a function of osteoclast number, compared with the *+/gm* osteoclasts (**Fig. 3D**).

Since it is known that the Rab-regulated endocytic pathway is crucial for formation of the ruffled border and resorption by osteoclasts, we examined the endocytic activity of *gm/gm* and *+/gm* macrophages by FACS analysis, using fluorescent conjugates of various endocytic markers. Endocytosis of dextran, a marker of fluid phase endocytosis, by *gm/gm* macrophages was significantly reduced by 60% compared with *+/gm* macrophages (**Fig. 4A**). By contrast, the uptake of wheat germ agglutinin and transferrin, markers of adsorptive endocytosis and receptor-mediated endocytosis respectively, was not significantly different between the *gm/gm* and *+/gm* macrophages (**Fig. 4B and C**). Using confocal microscopy, we confirmed this defect in fluid-phase endocytosis in the *gm/gm* osteoclasts, in which there was less uptake of FITC-dextran compared with the *+/gm* osteoclasts, and this appeared to be distributed more around the periphery of the osteoclasts (**Fig. 4D**). In addition, when we pre-incubated these

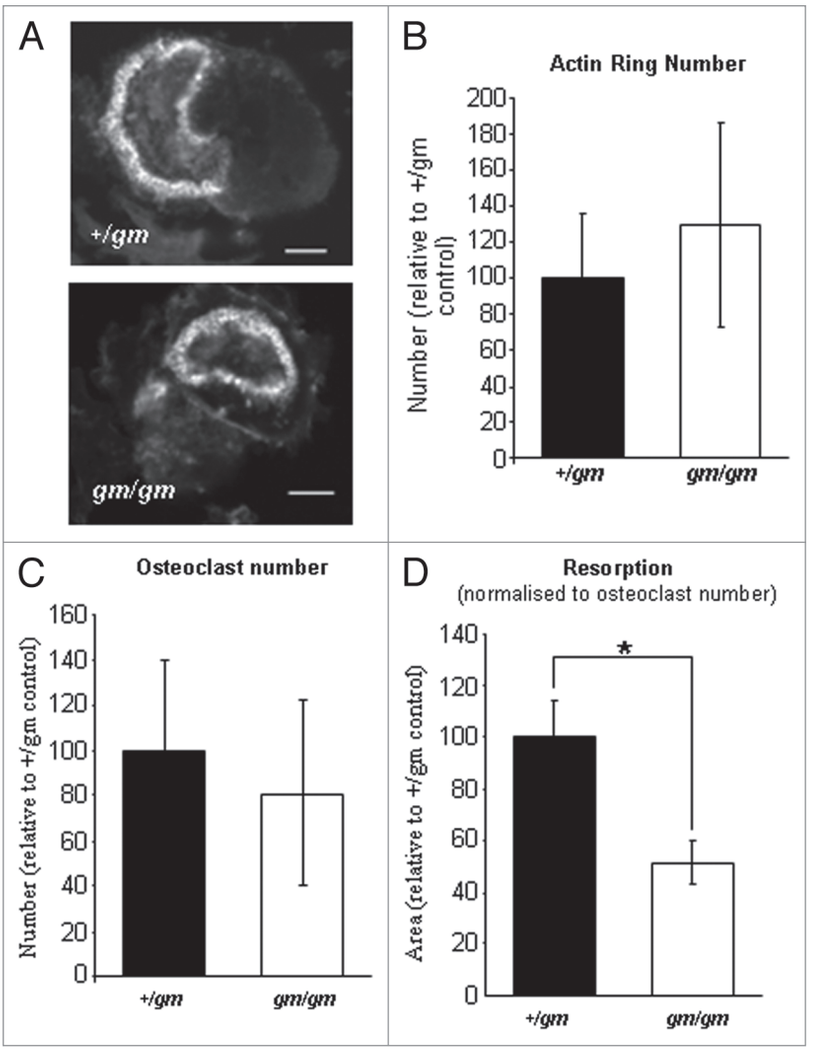


**Figure 3.** Osteoclasts generated from *gm/gm* mice in vitro have defective resorptive activity. Osteoclasts formed from *+/gm* and *gm/gm* marrow on dentine slices were assessed for their ability to become activated, as indicated by the presence of an actin ring (A). Actin ring number (B) and the number of osteoclasts per well (multinucleated TRAP-positive cell number) (C) were quantified for each culture. Resorption of the calcified substrate was quantified using reflected light microscopy and normalized to osteoclast number (D). Each experiment consisted of six replicates and the results shown are an average of three experiments ± SEM [*p < 0.05].

osteoclasts with a low concentration of the RGGT inhibitor 3-PEHPC, we found a clear further decrease in FITC-dextran uptake in the *gm/gm* osteoclasts, but little difference in the *+/gm* osteoclasts, consistent with our findings in macrophages.[12]

***gm/gm* mice have reduced bone mass despite reduced osteoclast resorption in vitro.** Given the reduced osteoclast activity observed in vitro, we expected the *gm/gm* mice to have a corresponding high bone mass (osteosclerotic) phenotype that is indicative of osteoclast dysfunction in vivo. However, μCT analysis of the trabecular bone in proximal tibiae of 12-week old female mice showed that rather than having an osteosclerotic phenotype, *gm/gm* mice had a mild osteopenia (reduced bone mass), with a bone volume around 25% lower than that in the *+/gm* mice (**Fig. 5A**). Although not individually significant, the slight reductions in trabecular thickness and trabecular number (**Fig. 5C and D**) most likely account for this reduction in bone volume. Furthermore, statistically significant increases in trabecular pattern factor (**Fig. 5E**) and structure model index (**Fig. 5F**) were observed in *gm/gm* tibiae, indicating that the trabecular bone is less well connected than in *+/gm* mice (more 'rod-like' and less 'plate-like'). μCT analysis of proximal tibiae from 28-week old mice demonstrated that the differences between *gm/gm* and *+/gm* mice were maintained, albeit to a lesser degree, and both genotypes had at least 20% less trabecular bone compared with their 12-week old counterparts (data not shown).

To determine if the apparent absence of a defect in osteoclast activity in vivo might be due to a compensatory mechanism, such as an increase in osteoclast number, histomorphometric analysis was performed. However, no significant differences in osteoclast numbers between *+/gm* and *gm/gm* tibiae were found (**Fig. 6**). Moreover, no differences were observed for any of the other measured parameters, including osteoid surface and width, active and total resorption surfaces and osteoblast numbers (**Fig. 6**).

To assess whether there were any changes in osteoclast morphology that might hint at dysfunction in vivo, we examined *+/gm* and *gm/gm* osteoclasts at the ultrastructural level. Ultrathin sections from ulna and radial bones from three *gm/gm* and three *+/gm* mice were analyzed by TEM. There was a reduced proportion of *gm/gm* osteoclasts with an extensively formed ruffled border (score = 4; only one out of 31 *gm/gm* osteoclasts compared with seven out of 38 *+/gm* osteoclasts; **Fig. 7**). However, the osteoclasts in the *gm/gm* mice were able to form well-defined ruffled borders; the number classed as having moderate ruffled borders (score = 3) was approximately the same as for *+/gm* mice, although there was an increased number of *gm/gm* osteoclasts with rudimentary ruffled borders (score = 2; 42% had this morphology, compared with 26% of the *+/gm* osteoclasts).

**Trabecular bone loss following ovariectomy is slightly reduced in *gm/gm* mice compared with *+/gm* mice.** It is possible that osteoclast activity in the *gm/gm* mice may be sufficient to maintain bone remodelling under normal physiological conditions, but unable to cope with a resorptive challenge that substantially increases the activity of the osteoclasts. To address this possibility, we performed ovariectomy (OVX) experiments, which mimic the menopause, increasing osteoclast activity by reducing endogenous estrogen levels that normally suppress resorption by osteoclasts.[22] Over the 4 week period after operation, OVX caused a 23% reduction in bone mass in the *+/gm* mice compared with sham-operated animals. OVX also caused a reduction in bone mass in *gm/gm* mice, but this was to a lesser

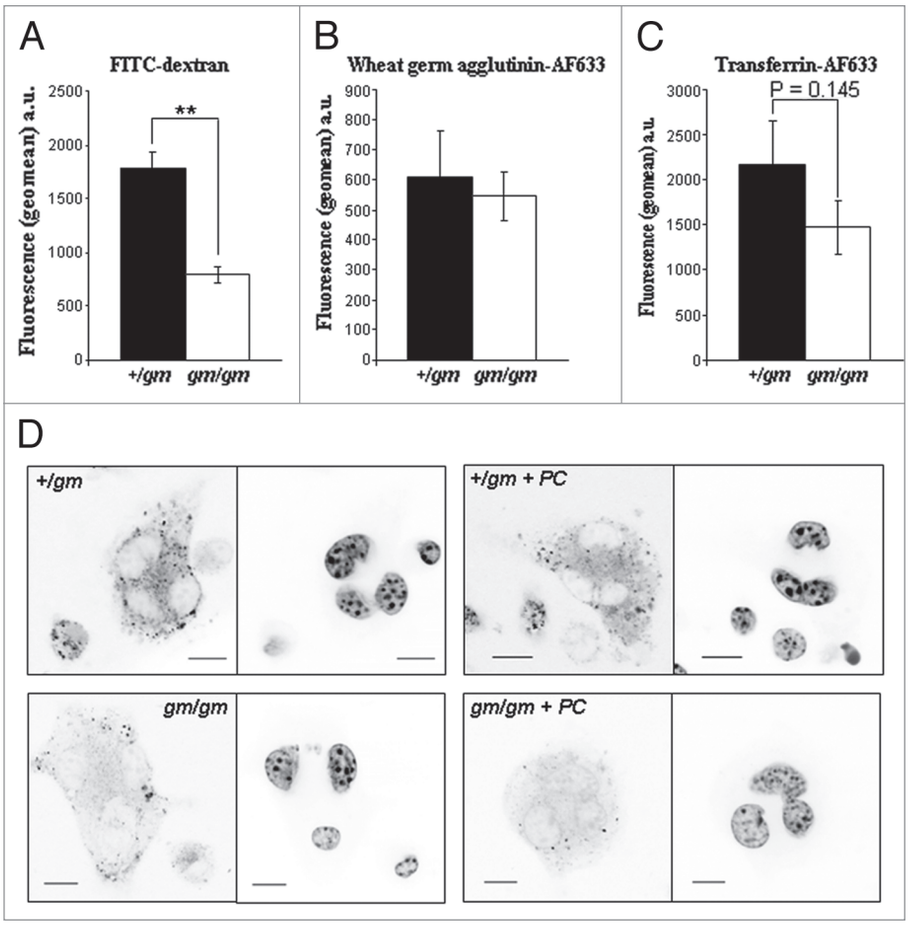


**Figure 4.** Fluid phase endocytosis is impaired in *gm/gm* macrophages and osteoclasts. Macrophages expanded from bone marrow were incubated with either (A) FITC-dextran (fluid phase endocytosis marker), (B) wheat germ agglutinin-633 (adsorptive endocytosis marker) or (C) transferrin-AF633 (receptor-mediated endocytosis marker) for 3 h. Uptake of the fluorescent compounds was detected by flow cytometry using a FACscalibur. Results are shown are the mean fluorescence intensity (geomean) averaged from 3 separate experiments ± SEM [**p < 0.01]. (D) Osteoclasts generated from *+/gm* and *gm/gm* mice were incubated with and without 0.1 mM 3-PEHPC for 24 h, together with 0.25 mg/ml FITC-dextran for the last 20 min, then fixed in paraformaldehyde and analyzed by confocal microscopy. One μm *xy* sections were captured using identical detector settings (optimised for the *+/gm* osteoclasts), and are displayed as inverted greyscale images. Left hand parts of the pairs show FITC dextran, right hand parts DAPI stain.

extent (by 14% compared with sham-operated mice; **Fig. 8**). In both the *+/gm* and *gm/gm* mice, these changes appear to be due to a combination of reduced trabecular number, and a concomitant increase in trabecular separation, rather than differences in trabecular thickness (**Fig. 8**).

**Osteoblasts from *gm/gm* mice accumulate unprenylated Rabs and exhibit impaired mineralization in vitro.** Since the reduced bone mass of *gm/gm* mice could not easily be explained by changes in osteoclast function, primary cultures of calvarial osteoblasts were studied in vitro to determine if reduced RGGT activity also affected the function of these bone-forming cells. Similar to osteoclasts, protein gel blot analysis showed the presence of unprenylated Rab2b and Rab3d in *gm/gm* osteoblasts, albeit to a much lesser extent than in the *gm/gm* osteoclasts (14%

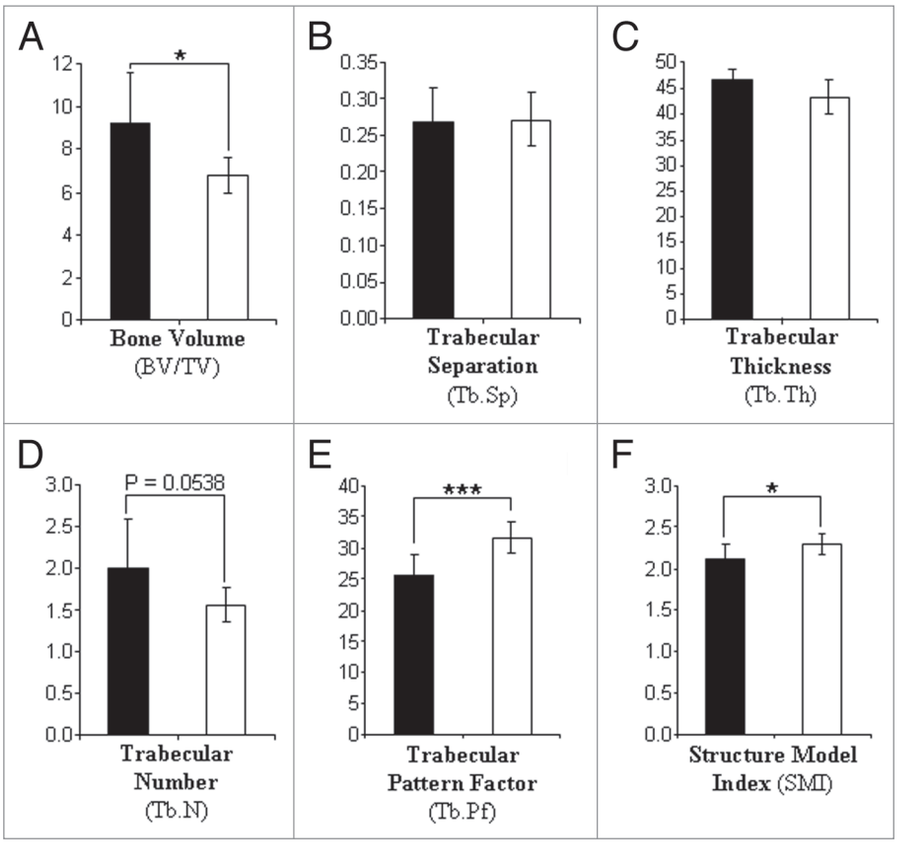


**Figure 5.** Trabecular bone volume is reduced in *gm/gm* tibiae. The tibiae from 12-week old mice were excised and analyzed by micro CT (resolution 5 μm). Quantitative analysis of 3D reconstructions (200 slices deep starting 20 slices down from the growth plate) was conducted to determine the bone volume, trabecular separation, trabecular thickness, trabecular number, trabecular pattern factor and structure model index. Results are the mean ± SD (n = 10 for *+/gm*; n = 8 for *gm/gm*). [*p < 0.05, ***p < 0.001; black bars = *+/gm*, white bars = *gm/gm*].

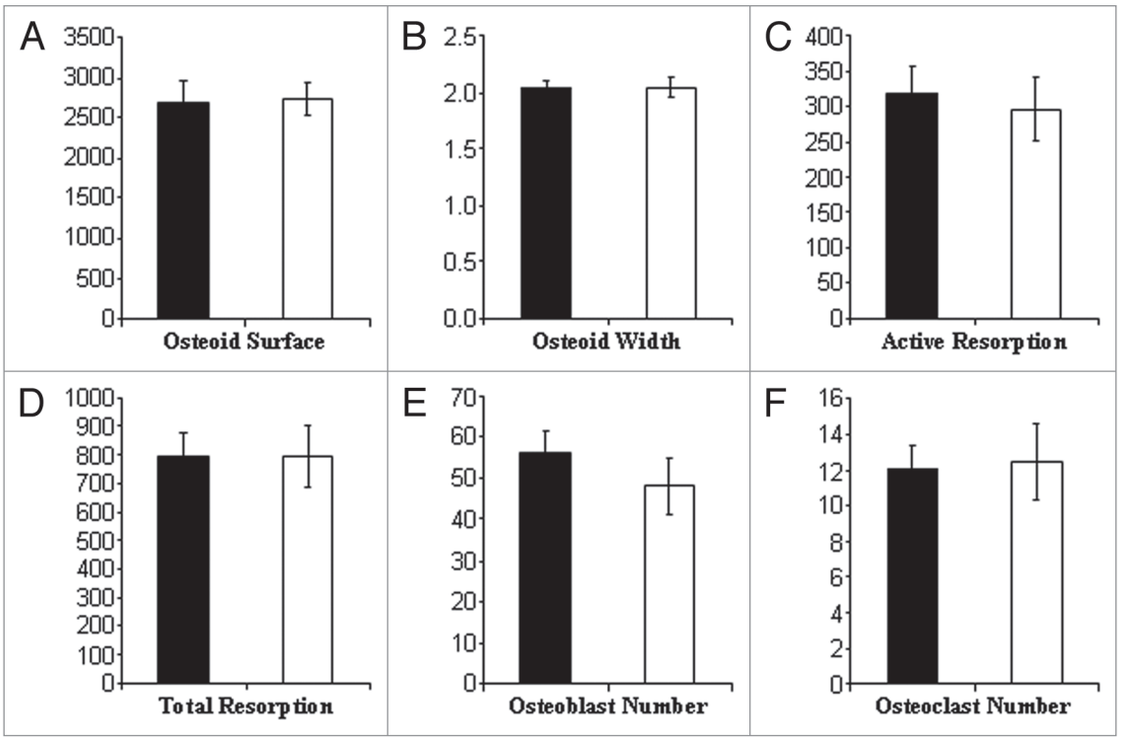


**Figure 6.** Histomorphometric parameters were unchanged in *gm/gm* tibiae. Tibia from 12-week old mice (previously analyzed by micro CT) were embedded in methylmethacrylate, sectioned and stained with Von Kossa and Paragon. Osteoid (A and B), resorption (C and D) and the number of osteoblasts and osteoclasts (E and F, respectively) were then quantified from sections at three depths through each bone. Results are the mean ± SD (n = 10 for *+/gm*; n = 8 for *gm/gm*). [black bars = *+/gm*, white bars = *gm/gm*].

and 37% in the unprenylated form, respectively), while Rab10 was exclusively in prenylated form (**Fig. 9A**). As expected, all these Rabs could be detected only in the prenylated form in the *+/gm* osteoblasts. However, in contrast to the *gm/gm* osteoclasts, no unprenylated Rab7 or Rab14 could be detected in the *gm/gm* osteoblasts, further indicating that although osteoblasts from the *gm/gm* mice have a prenylation defect, it is much less severe than in the *gm/gm* osteoclasts. To assess whether osteoblast function in the *gm/gm* mice was compromised, alkaline phosphatase activity assays were performed. In all cases stimulation with PTH or differentiation media for 48 h resulted in an increase in alkaline phosphatase activity for both *gm/gm* and *+/gm* osteoblasts, but no significant differences existed between the genotypes with either treatment (**Fig. 9B**). To test if mineralization rate was altered, osteoblasts from *gm/gm* and *+/gm* mice were treated with differentiation media for 7, 14 or 21 d prior to staining with Alizarin Red. While mineralization by *gm/gm* osteoblasts could be detected at all time points, and the amount of mineral increased over time, the extent of mineralization was consistently reduced compared with *+/gm* osteoblasts (**Fig. 9C and D**), indicating a functional defect in the *gm/gm* osteoblasts.

## Discussion

In this manuscript we demonstrate that there is a defect in Rab prenylation in both osteoclasts and osteoblasts derived from *gm/gm* mice, which bear an autosomal recessive mutation in the catalytic α subunit of RGGT. In osteoclasts, this defective Rab prenylation also leads to a functional defect, at least in vitro. Moreover, this supports our pharmacological data, in which inhibition of RGGT activity inhibits bone resorption by osteoclasts.[9,10,12] However, these mice actually had slightly lower bone mass than the *+/gm* mice, which is inconsistent with osteoclast dysfunction, suggesting that in vivo, Rab prenylation is sufficient to maintain normal physiological levels of bone resorption by osteoclasts. The defects in Rab prenylation and mineralization in bone-forming osteoblasts in vitro may help to explain this surprising bone phenotype.

Previous studies of specific cell types have identified defects in Rab prenylation in platelets, melanocytes and cytotoxic T cells of *gm/gm* mice only. Rab27a and Rab11 are both severely underprenylated in platelets and melanocytes,[16,23] while Rab4 is also underprenylated but to a lesser extent.[16] Rab1b is underprenylated in platelets, but not in melanocytes, and Rab6 prenylation is unaffected in either of these cell types. Moreover, Rab27a is also underprenylated in cytotoxic T cells, in which there at least two other unidentified Rabs that are also underprenylated.[23] Studies of other tissues failed to find defective prenylation of any of these Rab proteins in kidney, liver, heart, spleen, lung or brain.[16] In this study, we now identify two further cell types, osteoclasts and osteoblasts, in which Rab prenylation is defective in *gm/gm* mice. Osteoclasts are especially sensitive, displaying defective prenylation of Rab2b, Rab3d, Rab5, Rab6, Rab7, Rab11 and Rab14 to an extent matching the defects seen in platelets and melanocytes.[16]

However, the Rab prenylation defect is not universal, since Rab10 and Rab18 remained fully prenylated in osteoclasts from the *gm/gm* mouse. We could not detect Rab27 expression in osteoclasts (data not shown), which probably explains why, in the in vitro prenylation assay, underprenylated high molecular weight Rabs (~27 kDa; Rab27 is one of very few Rabs of this molecular weight) were much less apparent in the osteoclasts compared with PBMCs (**Fig. 1B**). In osteoblasts, fewer of the Rabs tested were affected, and even in the Rabs that were hypoprenylated (Rab2b and Rab3d), this was substantially less than the defect seen in the osteoclasts.

These studies therefore confirm previous observations that (1) different cell types are differentially affected by the reduced RGGT activity in the *gm/gm* mouse; and (2) that Rab proteins are differentially underprenylated in specific cell types derived from these mice. The explanation for these differences remains obscure, although it does not appear to be simply related to the expression level of the individual Rabs, since some Rabs that are highly expressed in platelets, such as Rab6, are not underprenylated in these cells.[16] Indeed, the defective prenylation of Rab6 in *gm/gm* osteoclasts is particularly interesting, since this Rab has not been found underprenylated in any other cell type from these mice.

Until now, the only functional defects observed in cells of the *gm/gm* mouse have been in melanocytes, megakaryocytes, platelets and cytotoxic T cells, all of which have been ascribed to the defective prenylation of Rab27a.[15,19,23,24] However, given the extent of the prenylation defect in *gm/gm* osteoclasts, it would seem likely that these cells also have a functional impairment. Despite this, we found that osteoclastogenesis was normal in cells isolated from the *gm/gm* mice, although further suppression of RGGT activity using phosphonocarboxylates did result in a dramatic inhibition of osteoclastogenesis in vitro,[12] suggesting that the residual RGGT activity in the *gm/gm* mice is only just sufficient to maintain osteoclastogenesis. Histomorphometric data also indicates that osteoclast formation is normal in the *gm/gm* mice in vivo, since osteoclasts numbers were similar to those found in the *+/gm* mice.

Resorption by osteoclasts is effected by the trafficking of vesicles carrying proteases and ion pumps to the ruffled border region, to enable degradation of collagen and dissolution of bone

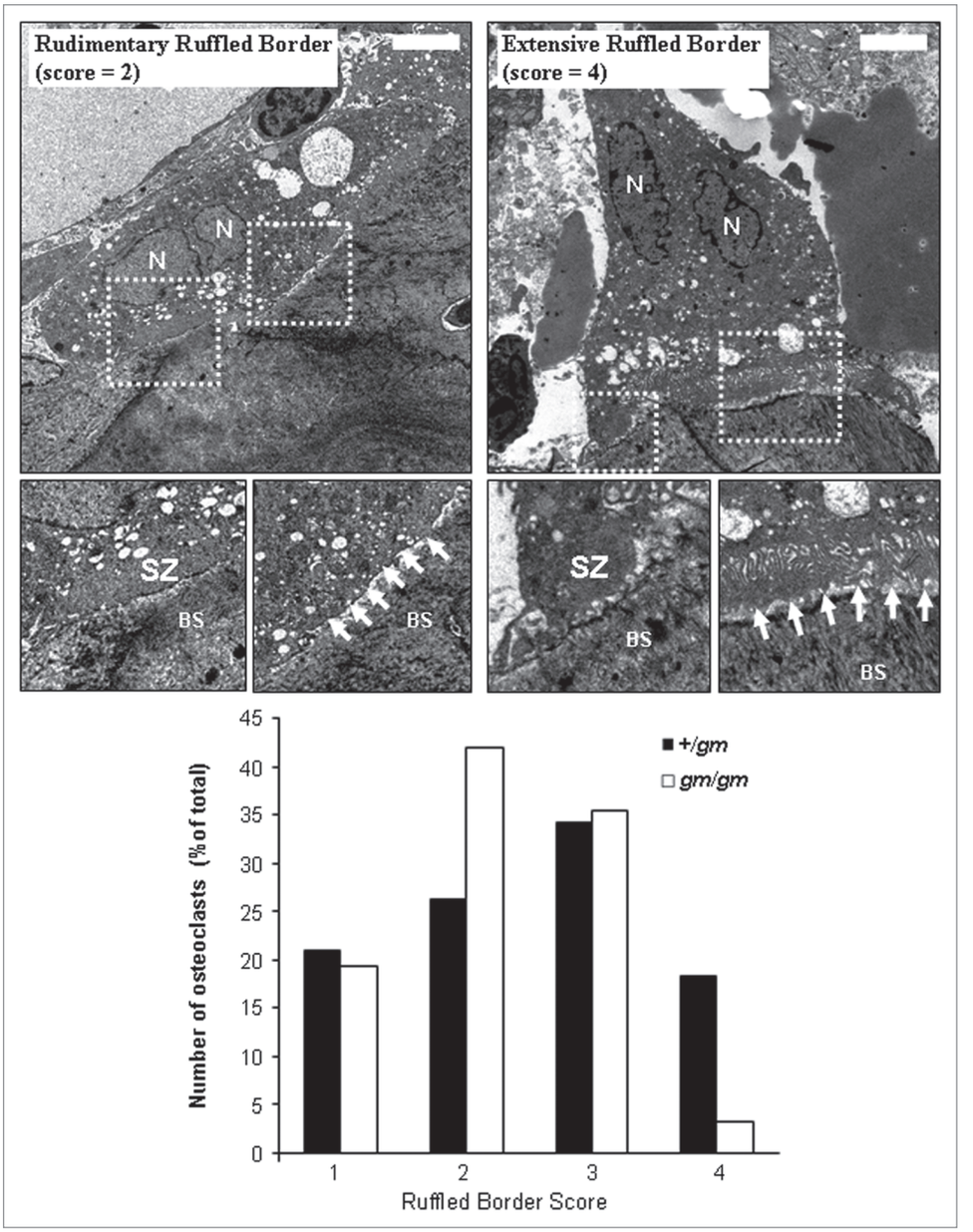


**Figure 7.** Ruffled borders are less well developed in *gm/gm* osteoclasts in vivo. Transmission electron micrographs of osteoclasts in the ulna or radius of *gm/gm* and *+/gm* mice were randomized and scored for ruffled border development according to the following criteria: score 1—no ruffled border apparent; score 2—rudimentary ruffled border, with poorly-developed membrane folds apparent; score 3—moderate ruffled border, with highly folded membrane apparent at some areas between sealing zones; score 4—extensive highly-folded ruffled border occupying entire area between sealing zones. Images show typical examples of a rudimentary (score 2) and extensive ruffled border (score 4); bar = 5 μm, N = nucleus, SZ = sealing zone, BS = bone surface. The number of osteoclasts exhibiting ruffled borders scored in each of the four categories is shown in the graph.

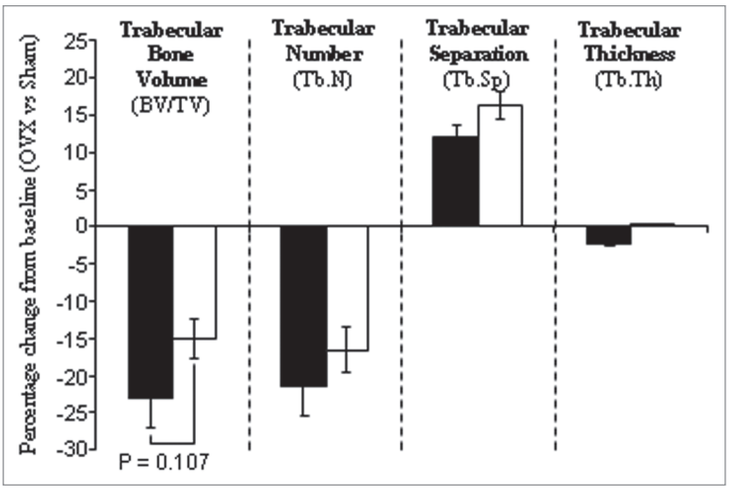


**Figure 8.** Trabecular bone loss following ovariectomy is slightly reduced in *gm/gm* mice. Eight-week old female *+/gm* and *gm/gm* mice were ovariectomized or sham-operated, then four weeks later the tibia were excised and analyzed by micro CT. Quantitative analysis of 3D reconstructions of the trabecular bone (200 slices deep starting 20 slices down from the growth plate) was conducted to determine trabecular bone volume, number, separation and thickness. The mean percentage change from sham-operated siblings is shown ± SD; n = 7. [black bars = *+/gm*, white bars = *gm/gm*].

mineral, respectively, a process that is dependent on prenylated Rab GTPases.[4] Accordingly, the resorptive activity of *gm/gm* osteoclasts in vitro was less than half that of *+/gm* osteoclasts, which is also consistent with the ability of phosphonocarboxylate inhibitors of RGGT to reduce osteoclastic resorption.[9,25] Two of the Rabs that were found to be underprenylated in the *gm/gm* osteoclasts, Rab3d and Rab7, have been ascribed crucial roles in osteoclastic resorption,[13,14] and are therefore likely candidates for causing this resorptive defect (Rab3d in particular, since the prenylation defect was much greater than that in Rab7). We also found that fluid-phase endocytosis is compromised in the *gm/gm* macrophages and osteoclasts, since they displayed defective uptake of fluorescent conjugates of dextran and the phosphonocarboxylate 3-PEHPC, which is also internalised by endocytosis.[12] Since the endocytic pathway is critical for osteoclastic resorption,[26] this suggests that compromised early endocytic pathways may be another potential contributor to the resorptive defect, in addition to Rab7-regulated late endocytic pathways; this could potentially be the result of the prenylation defect seen in Rab5, which regulates the early endocytic pathway.[27] Other evidence for defects in the endocytic pathway in $CD14^+$ monocytes under conditions of Rab under-prenylation come from studies of choroideremia patients who bear mutations in Rab escort protein-1; the lysosomal pH in monocytes from these patients is increased and proteolytic degradation impaired.[28]

Reorganization of the actin cytoskeleton is the first step in osteoclast activation and is a prerequisite for ruffled border formation and resorption by osteoclasts.[29] This process involves the formation of the actin ring, which comprises a dense clustering of podosomes that forms the sealing zone by which the osteoclast attaches tightly to the underlying extracellular matrix. We found that osteoclasts derived from *gm/gm* mice retained the ability to form actin rings, which is not surprising given that these structures are regulated by Rho family GTPases[30,31] that are prenylated by GGTase I rather than RGGT. This data is also consistent

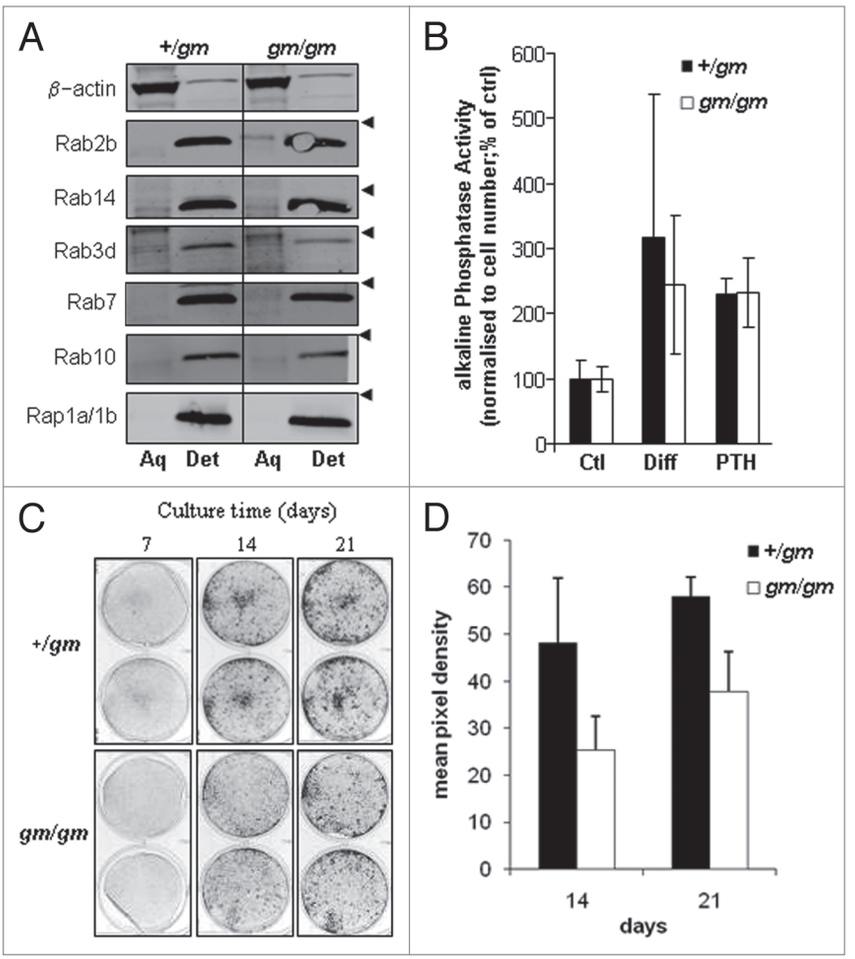


**Figure 9.** Rab GTPases are underprenylated in *gm/gm* osteoblasts. Calvarial osteoblasts from *gm/gm* and *+/gm* mice were lysed in triton X-114 buffer and fractionated into aqueous and detergent phases, enabling the separation of unprenylated and prenylated Rabs, respectively, which were detected by protein gel blotting; arrowheads indicate the position of the 28 kDa marker (A). Alkaline phosphatase activity in *gm/gm* and *+/gm* osteoblasts was detected following treatment with either differentiation media (β-glycerophosphate and ascorbic acid) or parathyroid hormone (B). Mineralization by *gm/gm* and *+/gm* osteoblasts cultured for 7, 14 and 21 d was assessed by staining with Alizarin Red (C) and the pixel densities (14 and 21 d) quantified and expressed as mean ± SD (D).

with the inability of pharmacological inhibition of RGGT to affect the actin cytoskeleton in osteoclasts.[9] Moreover, the overall phenotype of *gm/gm* osteoclasts is similar to that of osteoclasts generated from osteopetrotic patients, which bear mutations in the machinery responsible for lysosomal acidification or trafficking, including a protein that appears to be involved in Rab7-regulated late endosome/lysosome trafficking to the ruffled border.[32]

If the dysfunction that we found in *gm/gm* osteoclasts in vitro was mirrored in vivo, it would be expected that the *gm/gm* mice would have increased bone volume. However, μCT analysis revealed that the *gm/gm* mice actually had a slightly decreased bone volume at 12 weeks of age, and consistent with this a small decrease in trabecular number and increase in trabecular pattern factor. Moreover, analysis of osteoclast ultrastructure in vivo revealed that *gm/gm* osteoclasts were capable of forming ruffled borders, although the number of cells in which these were extensively developed was reduced compared with *+/gm* osteoclasts, suggesting that they may have a defect that only manifests itself under conditions of high bone turnover in which the activity of the osteoclasts is increased. Such a phenotype is seen in the β3 integrin knockout mouse; the osteoclasts have defective ruffled borders in vivo and reduced resorptive activity in vitro, but lack a bone phenotype at 2 mo of age.[22,33] However, these mice fail to respond to OVX, which increases osteoclast activity and induces bone loss in wild type mice due to the loss of the inhibitory effect of estrogen.[22] We therefore used a similar OVX approach to stimulate osteoclast-mediated bone resorption in the *gm/gm* mice. Since the resorptive response of *gm/gm* mice to OVX was significantly reduced compared with *+/gm* mice, it is indeed likely that there is a mild osteoclast dysfunction in the *gm/gm* mice that only becomes apparent under conditions of excessive resorption. These data suggest that other factors, such as increased osteoclast number,[33] or alterations to osteoblast number and/or activity, may compensate for reduced osteoclast function in vivo in the *gm/gm* mice under normal physiological conditions. However, histomorphometric analysis revealed no differences between the numbers of osteoclasts and osteoblasts in the proximal tibiae of *gm/gm* mice compared with the *+/gm* mice.

We therefore studied the in vitro phenotype of osteoblasts derived from the *gm/gm* mice, since a defect in these cells might contribute to the in vivo bone phenotype. Although the Rab prenylation defect was much milder in these cells than in the *gm/gm* osteoclasts, the *gm/gm* osteoblasts were defective in mineralization assays in vitro. The trafficking of matrix vesicles to the cell surface in osteoblasts is essential for the process of bone formation and mineralization. These vesicles express numerous Rabs, including Rab7, Rab6 and Rab2;[34] we found that Rab2b was underprenylated in *gm/gm* osteoblasts, offering a potential explanation for this mineralization defect. Recently, Rab27 has been shown to be expressed in osteoblasts at the mRNA level.[35] Given that the defects in function of platelets, melanocytes and cytotoxic T cells in *gm/gm* mice have all been ascribed to defective Rab27 prenylation,[15,23,24] it is also possible that defective prenylation of this Rab could be responsible, at least in part, for the mineralization defect in osteoblasts. However, this is complicated by the fact that Rab27 appears to be involved in trafficking of the osteoclastogenic cytokine RANKL to the cell surface in osteoblasts,[35] in which case impaired Rab27 function would be expected to reduce osteoclast number, which we found no evidence for in vivo. Therefore, we attempted to assess the prenylation status of Rab27a in *gm/gm* osteoblasts, but surprisingly we were unable to detect this Rab in mouse osteoblasts (data not shown).

Defects in other cell types may also affect bone turnover in the *gm/gm* mice. Megakaryocytes are known to be dysfunctional in *gm/gm* mice, leading to reduced platelet formation.[19] Furthermore, megakaryocytes can inhibit osteoclastogenesis and resorption in vitro in mouse and human coculture experiments,[36,37] which may be the result of their expression of the soluble RANKL decoy receptor osteoprotegerin (OPG).[38] It is therefore possible that in the *gm/gm* mice, Rabs involved in trafficking of OPG are underprenylated, thus resulting in reduced OPG secretion and increased osteoclast activity, potentially accounting for the slight bone loss that was found in the *gm/gm* mice.

In conclusion, we have demonstrated a significant Rab prenylation defect in both osteoclasts and osteoblasts in the *gm/gm* mice, which was particularly profound in the former. This leads to a functional deficit in both these cell types in vitro, which can therefore be added to the restricted number of cell types known to be affected in *gm/gm* mice, namely platelets, melanocytes, megakaryocytes and cytotoxic T cells. Further studies are required to identify the individual Rab proteins whose compromised prenylation produces the functional deficit in osteoclasts and osteoblasts in vitro, and to fully explain the mild in vivo bone phenotype of these mice, which is likely the result of a multitude of factors, rather than a functional deficit in a single cell type.

## Materials and Methods

**Animals.** *Gunmetal* mice were housed in a designated animal facility and given ad libitum access to food and water. All experiments with animals were approved under UK. Home Office regulations.

**Culture of osteoclasts and osteoblasts from *gm/gm* mice.** *Osteoclast cultures:* Marrow was flushed from mouse hindlimb long-bones into Dulbecco modified eagles medium α-formulation (α-MEM; Sigma) supplemented with 10% fetal calf serum (FCS), 1 mM L-glutamine, 100 U/ml penicillin and 100 μg/ml streptomycin. A single-cell suspension was achieved by gently passing the media through 19 G and 22 G needles. After incubation overnight at 37°C (5% $CO_2$), the non adherent cells were isolated, and red blood cell contamination eliminated using PharmLyse™ (BD Biosciences) in accordance with the manufacturers instruction. The cell suspension was then incubated with 25 ng/ml mouse macrophage colony stimulating factor (mM-CSF; R&D Systems, UK) for 48 h to promote monocyte proliferation. To generate osteoclasts, expanded monocytes were transferred onto dentine or plastic in 96-well plates ($1.5 \times 10^4$/well) and incubated with 50 ng/ml mM-CSF and 20 ng/ml human receptor activator of NFκB ligand (hRANKL; R&D Systems). Media was replaced every 48 h until osteoclasts

had formed (5–7 d). *Osteoblast cultures:* Calvarial osteoblasts were isolated from the calvariae of neonatal *+/gm* or *gm/gm* mice using collagenase/EDTA as described previously in reference 39.

**Assay for endogenous RGGT activity.** Twenty micrograms of cytosolic protein from osteoclasts generated from *gm/gm* or *+/gm* mice was added to a 25 μl reaction containing 50 mM sodium Hepes (pH 7.2), 5 mM $MgCl_2$, 1 mM DTT, 50 uM NP-40, 1 μM [$^3$H]GGPP (47,300 dpm/pmol), 0.5 μM recombinant Rab Escort Protein1 and 0.5 μM recombinant Rab1 protein. The reactions were allowed to proceed for 30 min at 37°C, after which sample buffer was added and the entire contents of the reaction electrophoresed on a 17.5% SDS-polyacrylamide gel. Gels were then fixed, soaked in AMPLIFY solution (Amersham Biosciences) for 20 min, dried and exposed to MP Hyperfilm for 1 mo. [$^3$H] incorporation was visualized using a Cyclone PhophorImaging system (PerkinElmer).

**Determining the prenylation status of Rab proteins in vitro.** To detect unprenylated Rab GTPases within the cells, the assay was run as above, substituting 0.5 μM recombinant RGGT in place of recombinant Rab1. To examine the prenylation status of Rab proteins by protein gel blotting, triton X-114 fractionation was used to separate the prenylated and unprenylated forms of Rabs in whole cell lysates, as previously described in reference 10. Subcellular localization of Rab6 in *gm/gm* and *+/gm* osteoclasts was detected by immunostaining as described previously in reference 40. In order to assess the percentage of each Rab GTPase that was in the unprenylated form, the intensity of each band was quantified using ImageJ software.

**Assessment of osteoclast formation and activity in vitro.** Osteoclasts were generated from the bone marrow of *gm/gm* and *+/gm* mice on dentine discs. Forty-eight hours after osteoclast formation was first detected visually (typically after 5–7 d treatment with RANKL), the dentine slices were fixed in 4% formaldehyde and formation and activity of the osteoclasts assessed as described previously in reference 9.

**Determining the endocytic activity of *gm/gm* macrophages and osteoclasts.** Bone-marrow derived macrophages or osteoclasts from *gm/gm* or *+/gm* mice were incubated with tetramethylrhodamine-dextran or FITC-dextran (250 μg/ml), transferrin-AF633 (20 μg/ml) or wheat germ agglutinin-AF633 (5 μg/ml) (all from Invitrogen) for 3 h (macrophages) or 20 min (osteoclasts). In some cases the osteoclasts were also incubated with the RGGT inhibitor 3-PEHPC (0.1 mM) for 24 h prior to incubation with FITC-dextran. Macrophage cultures were washed three times in PBS, then detached from the plate using trypsin and fixed in 1% paraformaldehyde. The uptake of each endocytic tracer was quantified by FACS using a Facscalibur (BD Biosciences). After establishing baseline fluorescence using untreated macrophages from each genotype, the geo-mean fluorescence was calculated and used as the measure for uptake. Ten thousand events were recorded for each sample. Osteoclast cultures were washed three times in PBS, fixed in 4% paraformaldehyde, then mounted on to glass slides in VectShield and analyzed by confocal microscopy using a Zeiss LSM700.

**Assessment of the bone phenotype of *gm/gm* mice using microCT.** Female *gm/gm* and heterozygous mice were analyzed at 12 weeks of age, four weeks after undergoing either ovariectomy (OVX) or sham operation. For sham operated animals the ovaries were inspected in situ prior to suturing the wounds. In the case of OVX operated animals the ovaries and fat pad were removed with scissors and the fallopian tubes tied with surgical thread. Animals were housed for a further four weeks, after which time the animals were sacrificed (i.e., 12 weeks of age) and the long bones removed for analysis. Three-dimensional analysis of proximal tibiae was performed on a SkyScan-1072 high-resolution desktop micro-CT system (Skyscan). The right tibia from each animal was scanned through 180° (in 0.68° increments with a 6.5 sec acquisition time) with a pixel size of 5.05 μm using a 0.5 mm aluminum filter. Two hundred slices of trabecular region (corresponding to a depth of 1 mm) were selected distal to the epiphyseal growth plate, and cortical bone was excluded from the region of interest. Three-dimensional reconstructions of each bone were made using NRecon software and analysis of morphometric parameters was performed using CTAn software (Skyscan).

**Bone histomorphometry.** Following μCT scanning, the tibiae were embedded in methylmethacrylate resin and semi-thin sections cut to give three transverse sections at ¼, ½ and ¾ depths through the bone. The resin was removed from each section with xylene (20 min) prior to Von Kossa staining (1.5% Silver nitrate; 5 min in the dark followed by reducing in 0.5% hydroquinone). Each section was also counterstained with paragon for 2 min before drying on a hotplate (60°C) and a final clean in xylene. Histomorphometric quantification of osteoid surface, active resorption surface, total resorption surface, osteoblast number and osteoclast number was performed for each of the three sections from each tibia. Data used for analysis was an average of the three sections for each tibia.

**Analysis of osteoclast ruffled borders in vivo by TEM.** The ulna and radial bones were removed from 12-week old *gm/gm* and *+/gm* mice and fixed in 2.5% glutaraldehyde containing 0.1 M cacodylate for 24 h. The bones were then decalcified by replenishing with fixative supplemented with 2.5% EDTA (w/v). The decalcifying fixative was replenished twice a week for two weeks, after which the bones were trimmed and the growth plate region retained for embedding. The bones were post-fixed in 1% osmium tetroxide and dehydrated in increasing concentrations of ethanol (35% to 100% over 2 h). The bones were then infiltrated with Epon resin (Miller-Stephenson Chemicals) and cured at 60°C overnight. Ultra-thin sections (70 nm) were cut through the growth plate region using a diamond knife fitted in a Leica Ultramicrotome UC6. Sections were transferred to copper grids and stained with uranyl acetate and lead citrate to improve contrast, before being observed using a Philips CM10 transmission electron microscope (TEM). Samples were blinded, then images of every osteoclast observed were taken and the ruffled border morphology in osteoclasts in which sealing zones could be identified was scored according to the criteria outlined in **Figure 7**.

**Analysis of *gm/gm* osteoblasts in vitro.** In vitro alkaline phophatase activity was quantified as a marker of osteoblast maturation. Briefly, osteoblasts seeded in 96-well plates at 1 x $10^4$ cells per well were first treated with 40 nM parathyroid hormone

(PTH), differentiation media (10 mM β-glycerophopshate and 5 mg/ml ascorbic acid) or untreated media for 48 h, before being lysed in 150 μl of ice-cold 1 M diethanolamine containing 1 mM $MgCl_2$ and 0.05% Triton. 50 μl of each lysate was incubated with 50 μl of 20 mM para-nitrophenol-phosphate (in 1 M diethanolamine; 1 mM $MgCl_2$) at 37°C for 30 min in a Synergy HT BioTek plate reader; absorbance at 414 nm was measured every 2 min. Enzyme activity ($V_{max}$) was calculated using a nitrophenol standard curve (0–30 nmol per well) as an indirect measure of the enzyme expression level. Mineralization was assessed in calvarial osteoblasts seeded in 6-well plates and incubated with differentiation media (see above) for 7, 14 or 21 d. After fixation in cold 70% ethanol the calcium-rich mineral was stained with Alizarin Red. Stained mineral was imaged using a flat bed scanner set to color positive film and using a backlight. Mean pixel density was quantified from each well of these images using ImageJ software.

**Statistical analysis.** Data from three or more in vitro experiments was collated and expressed as mean ± SEM. Data from μCT and histomorphometric analysis was expressed as mean ± SD. Experimental differences between *gm/gm* and *+/gm* tissues were analyzed for statistical significance using an unpaired t-test.


### Acknowledgments

We would like to thank Dr. Anke Roelofs and Dr. Keith Thompson for assistance with the FACS analysis. This work was supported by the Scottish Hospital Endowments Research Trust (SHERT), a studentship to A.T. from the Nuffield Foundation's Oliver Bird Rheumatism Programme, the Cunningham Trust for assistance with TEM, Arthritis Research UK (Programme Grant ARUK17285) for general technical support and the Wellcome Trust.


### References


1. Boyle WJ, Simonet WS, Lacey DL. Osteoclast differentiation and activation. Nature 2003; 423:337-42; PMID: 12748652; DOI:10.1038/nature01658.
2. Yoshida H, Hayashi SI, Kunisada T, Ogawa M, Nishikawa S, Okamura H, et al. The murine mutation osteopetrosis is in the coding region of the macrophage colony stimulating factor gene. Nature 1990; 345:442-4; PMID: 2188141; DOI:10.1038/345442a0.
3. Udagawa N, Takahashi N, Jimi E, Matsuzaki K, Tsurukai T, Itoh K, et al. Osteoblasts/stromal cells stimulate osteoclast activation through expression of osteoclast differentiation factor/RANKL but not macrophage colony-stimulating factor: receptor activator of NFkappaB ligand. Bone 1999; 25:517-23; PMID: 10574571.
4. Coxon FP, Taylor A. Vesicular trafficking in osteoclasts. Semin Cell Dev Biol 2008; 19:424-33; PMID: 18768162; DOI:10.1016/j.semcdb.2008.08.004.
5. Dunford JE, Thompson K, Coxon FP, Luckman SP, Hahn FM, Poulter CD, et al. Structure-Activity Relationships for Inhibition of Farnesyl Diphosphate Synthase in Vitro and Inhibition of Bone Resorption in Vivo by Nitrogen-Containing Bisphosphonates. J Pharmacol Exp Ther 2001; 296:235-42; PMID: 11160603.
6. Kavanagh KL, Guo KD, Dunford JE, Wu XQ, Knapp S, Ebetino FH, et al. The molecular mechanism of nitrogen-containing bisphosphonates as anti osteoporosis drugs. Proc Natl Acad Sci USA 2006; 103:7829-34; PMID: 16684881; DOI:10.1073/pnas.0601643103.
7. Coxon FP, Thompson K, Rogers MJ. Recent advances in understanding the mechanism of action of bisphosphonates. Curr Opin Pharmacol 2006; 6:307-12; PMID: 16650801; DOI:10.1016/j.coph.2006.03.005.
8. Rogers MJ, Crockett JC, Coxon FP, Monkkonen J. Biochemical and molecular mechanisms of action of bisphosphonates. Bone 2010; In press; PMID: 21111853; DOI:10.1016/j.bone.2010.11.008.
9. Coxon FP, Helfrich MH, Larijani B, Muzylak M, Dunford JE, Marshall D, et al. Identification of a novel phosphonocarboxylate inhibitor of Rab geranylgeranyl transferase that specifically prevents Rab prenylation in osteoclasts and macrophages. J Biol Chem 2001; 276:48213-22; PMID: 11581260.
10. Coxon FP, Ebetino FH, Mules EH, Seabra MC, McKenna CE, Rogers MJ. Phosphonocarboxylate inhibitors of Rab geranylgeranyl transferase disrupt the prenylation and membrane localization of Rab proteins in osteoclasts in vitro and in vivo. Bone 2005; 37:349-58; PMID: 16006204; DOI:10.1016/j.bone.2005.04.021.
11. McKenna CE, Kashemirov BA, Blazewska KM, Mallard-Favier I, Stewart CA, Rojas J, et al. Synthesis, chiral high performance liquid chromatographic resolution and enantiospecific activity of a potent new geranylgeranyl transferase inhibitor, 2-hydroxy-3-imidazo[1,2-a]pyridin-3-yl-2-phosphonopropionic acid. J Med Chem 2010; 53:3454-64; PMID: 20394422; DOI:10.1021/jm900232u.
12. Coxon FP, Taylor A, Stewart CA, Baron R, Seabra MC, Ebetino FH, et al. The *gunmetal* mouse reveals Rab geranylgeranyl transferase to be the major molecular target of phosphonocarboxylate analogues of bisphosphonates. Bone 2011; In press; PMID: 21419243; DOI:10.1016/j.bone.2011.03.686.
13. Zhao H, Laitala-Leinonen T, Parikka V, Vaananen HK. Downregulation of small gtpase rab7 impairs osteoclast polarization and bone resorption. J Biol Chem 2001; 276:39295-302; PMID: 11514537; DOI:10.1074/jbc.M010999200.
14. Pavlos NJ, Xu J, Riedel D, Yeoh JS, Teitelbaum SL, Papadimitriou JM, et al. Rab3d regulates a novel vesicular trafficking pathway that is required for osteoclastic bone resorption. Mol Cell Biol 2005; 25:5253-69; PMID: 15923639; DOI:10.1128/MCB.25.12.5253-69.2005.
15. Detter JC, Zhang Q, Mules EH, Novak EK, Mishra VS, Li W, et al. Rab geranylgeranyl transferase alpha mutation in the gunmetal mouse reduces Rab prenylation and platelet synthesis. Proc Natl Acad Sci USA 2000; PMID: 10737774; DOI:10.1073/pnas.080517697.
16. Zhang Q, Zhen L, Li W, Novak EK, Collinson LM, Jang EK, et al. Cell-specific abnormal prenylation of Rab proteins in platelets and melanocytes of the gunmetal mouse. Br J Haematol 2002; 117:414-23; PMID: 11972527; DOI:10.1046/j.1365-2141.2002.03444.x.
17. Tiwari S, Italiano JE Jr, Barral DC, Mules EH, Novak EK, Swank RT, et al. A role for Rab27b in NF-E2-dependent pathways of platelet formation. Blood 2003; 102:3970-9; PMID: 12907454; DOI:10.1182/blood-2003-03-0977.
18. Swank RT, Jiang SY, Reddington M, Conway J, Stephenson D, McGarry MP, et al. Inherited abnormalities in platelet organelles and platelet formation and associated altered expression of low molecular weight guanosine triphosphate-binding proteins in the mouse pigment mutant gunmetal. Blood 1993; 81:2626-35; PMID: 8490171.
19. Novak EK, Reddington M, Zhen L, Stenberg PE, Jackson CW, McGarry MP, et al. Inherited thrombocytopenia caused by reduced platelet production in mice with the gunmetal pigment gene mutation. Blood 1995; 85:1781-9; PMID: 7703484.
20. Larijani B, Hume AN, Tarafder AK, Seabra MC. Multiple factors contribute to inefficient prenylation of Rab27a in Rab prenylation diseases. J Biol Chem 2003; 278:46798-804; PMID: 12941939; DOI:10.1074/jbc.M307799200.
21. Raposo G, Marks MS, Cutler DF. Lysosome-related organelles: driving post-Golgi compartments into specialisation. Curr Opin Cell Biol 2007; 19:394-401; PMID: 17628466; DOI:10.1016/j.ceb.2007.05.001.
22. Zhao H, Kitaura H, Sands MS, Ross FP, Teitelbaum SL, Novack DV. Critical role of beta 3 integrin in experimental postmenopausal osteoporosis. J Bone Miner Res 2005; 20:2116-23; PMID: 16294265; DOI:10.1359/JBMR.050724.
23. Stinchcombe JC, Barral DC, Mules EH, Booth S, Hume AN, Machesky LM, et al. Rab27a is required for regulated secretion in cytotoxic T lymphocytes. J Cell Biol 2001; 152:825-34; PMID: 11266472; DOI:10.1083/jcb.152.4.825.
24. Hume AN, Collinson LM, Rapak A, Gomes AQ, Hopkins CR, Seabra MC. Rab27a regulates the peripheral distribution of melanosomes in melanocytes. J Cell Biol 2001; 152:795-808; PMID: 11266470; DOI:10.1083/jcb.152.4.795.
25. Ebetino FH, Bayless AV, Ambugey JI, Ibbotsen KJ, Dansereau S, Ebrahiimpour A. Elucidation of a pharmacophore for the bisphosphonate mechanism of antiresorptive activity. Phosphorus Sulfur Silicon Relat Elem 1996; 109-110:217-20.
26. Mulari MTK, Zhao H, Lakkakorpi PT, Vaananen HK. Osteoclast ruffled border has distinct subdomains for secretion and degraded matrix uptake. Traffic 2003; 4:113-25; PMID: 12559037; DOI:10.1034/j.1600-0854.2003.40206.x.
27. Bucci C, Parton RG, Mather IH, Stunnenberg H, Simons K, Hoflack B, et al. The Small Gtpase Rab5 Functions As A Regulatory Factor in the Early Endocytic Pathway. Cell 1992; 70:715-28; PMID: 1516130; DOI:10.1016/0092-8674(92)90306-W.
28. Strunnikova NV, Barb J, Sergeev YV, Thiagarajasubramanian A, Silvin C, Munson PJ, et al. Loss-of-function mutations in Rab escort protein 1 (REP-1) affect intracellular transport in fibroblasts and monocytes of choroideremia patients. PLoS ONE 2009; 4:8402; PMID: 20027300; DOI:10.1371/journal.pone.0008402.
29. Mulari M, Vaaraniemi J, Vaananen HK. Intracellular membrane trafficking in bone resorbing osteoclasts. Microsc Res Tech 2003; 61:496-503; PMID: 12879417; DOI:10.1002/jemt.10371.
30. Ory S, Brazier H, Pawlak G, Blangy A. Rho GTPases in osteoclasts: Orchestrators of podosome arrangement. Eur J Cell Biol 2008; 87:469-77; PMID: 18436334; DOI:10.1016/j.ejcb.2008.03.002.

31. Itzstein C, Coxon FP, Rogers MJ. The regulation of osteoclast polarisation, function and survival by the Ras superfamily of GTPases. small GTPases 2011; In press.
32. Van Wesenbeeck L, Odgren PR, Coxon FP, Frattini A, Moens P, Perdu B, et al. Involvement of PLEKHM1 in osteoclastic vesicular transport and osteopetrosis in incisors absent rats and humans. J Clin Invest 2007; 117:919-30; PMID: 17404618; DOI:10.1172/JCI30328.
33. McHugh KP, Hodivala-Dilke K, Zheng MH, Namba N, Lam J, Novack D, et al. Mice lacking beta3 integrins are osteosclerotic because of dysfunctional osteoclasts. J Clin Invest 2000; 105:433-40; PMID: 10683372; DOI:10.1172/JCI8905.
34. Xiao Z, Camalier CE, Nagashima K, Chan KC, Lucas DA, de la Cruz MJ, et al. Analysis of the extracellular matrix vesicle proteome in mineralizing osteoblasts. J Cell Physiol 2007; 210:325-35; PMID: 17096383; DOI:10.1002/jcp.20826.
35. Kariya Y, Honma M, Hanamura A, Aoki S, Ninomiya T, Nakamichi Y, et al. Rab27a and Rab27b are involved in stimulation-dependent RANKL release from secretory lysosomes in osteoblastic cells. J Bone Miner Res 2011; 26:689-703; PMID: 20939018; DOI:10.1002/jbmr.268.
36. Kacena MA, Shivdasani RA, Wilson K, Xi Y, Troiano N, Nazarian A, et al. Megakaryocyte-osteoblast interaction revealed in mice deficient in transcription factors GATA-1 and NF-E2. J Bone Miner Res 2004; 19:652-60; PMID: 15005853; DOI:10.1359/JBMR.0301254.
37. Beeton CA, Bord S, Ireland D, Compston JE. Osteoclast formation and bone resorption are inhibited by megakaryocytes. Bone 2006; 39:985-90; PMID: 16870519; DOI:10.1016/j.bone.2006.06.004.
38. Chagraoui H, Sabri S, Capron C, Villeval JL, Vainchenker W, Wendling F. Expression of osteoprotegerin mRNA and protein in murine megakaryocytes. Exp Hematol 2003; 31:1081-8; PMID: 14585373; DOI:10.1016/S0301-472X(03)00233-9.
39. Armour KE, Armour KJ, Gallagher ME, Godecke A, Helfrich MH, Reid DM, et al. Defective bone formation and anabolic response to exogenous estrogen in mice with targeted disruption of endothelial nitric oxide synthase. Endocrinology 2001; 142:760-6; PMID: 11159848; DOI:10.1210/en.142.2.760.
40. Taylor A, Rogers MJ, Tosh D, Coxon FP. A novel method for efficient generation of transfected human osteoclasts. Calcif Tissue Int 2007; 80:132-6; PMID: 17308995; DOI:10.1007/s00223-006-0245-6.